Thermochimica Acta, 156 (1989) 211–224
Elsevier Science Publishers B.V., Amsterdam – Printed in The Netherlands

THE PbO_2–PbO–V_2O_5 SYSTEM IN AIR

Y.M. KASSEM, A.N. MAHDY and M.F. ABADIR

Chemical Engineering Department, College of Engineering, Cairo University, Giza (Egypt)

(Received 17 January 1989)

ABSTRACT

The equilibrium relationship in air of the system PbO_2–PbO–V_2O_5 was studied using the thermobalance technique, as well as combined TG–DTA and X-ray analysis. Three compounds were established: $2PbO \cdot V_2O_5$, $3PbO \cdot V_2O_5$ and $8PbO \cdot V_2O_5$. $4PbO \cdot V_2O_5$, was, however, not detected. $2PbO \cdot V_2O_5$ can be prepared from PbO_2 at a relatively low temperature (420 °C). The X-ray pattern for the compound $8PbO \cdot V_2O_5$ is presented and the compatible phases were established.

INTRODUCTION

The study of the phase equilibria of this system has been motivated by the increased importance of lead vanadate compositions in various fields of applications. Table 1 shows the various applications for glasses containing V_2O_5 and lead oxides. In addition, V_2O_5 has been recently extensively used

TABLE 1

Applications of PbO–V_2O_5 glasses

No.	Composition of glass	Use	Reference
1	PbO–V_2O_5	Heat resistant glass	1
		n-type semi-conductor	2
2	PbO–V_2O_5–B_2O_3	Low melting glass for composite materials	3 4
		Sealing glass ceramics and metallic parts	5
		Increasing the absorption of visible light	6
		Piezoelectric	7
3	PbO–V_2O_5–CuO	Vitreous semi-conductors	8

0040-6031/89/$03.50

with other oxides in the glass industry, particularly in glasses with special electrical properties [9,10].

PREVIOUS WORK

Lead vanadates

Various lead vanadates have been reported. Table 2 summarizes the available data.

The binary system Pb–O

This system had been previously reported by Abadir et al. [17].

The PbO–V_2O_5 system

Amadori [12] has published the phase diagram in Fig. 1 which shows the presence of 3 intermediate compounds melting congruently without evidence

TABLE 2

Lead vanadates

Compound	PbO : V_2O_5 (molar)	Properties	References
$2PbO \cdot V_2O_5$	2 : 1	Congruently melting at 721°C	11,12 13,14
$3PbO \cdot V_2O_5$	3 : 1	Hexagonal	15,16
		Congruently melting at 957°C	11,12
$4PbO \cdot V_2O_5$	4 : 1	Incongruently melting	16
$8PbO \cdot V_2O_5$	8 : 1	Monoclinic	16
		Has an allotropic transition at 775°C	14,11
		and congruently melting at 797°C	12

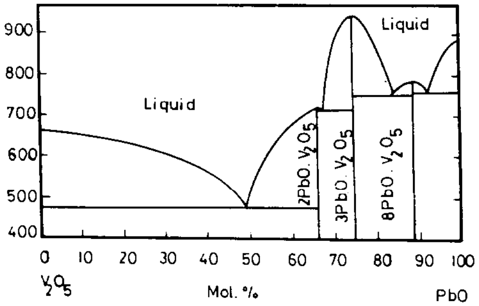

Fig. 1. PbO–V_2O_5 system, published by Amadori [12].

of any solid solubility. While $2PbO \cdot V_2O_5$ melts at 721 °C, $3PbO \cdot V_2O_5$ melts at 957 °C and $8PbO \cdot V_2O_5$ melts at 797 °C. The presence of these compounds was recently confirmed by several authors [16,18]. Their preparation from PbO and V_2O_5 required relatively high temperatures (600–750 °C) and long heating periods ranging from 1 day to 1 week. The compound $4\ PbO \cdot V_2O_5$ was reported by Shimohira et al. [16] and is not shown in Fig. 1.

In the present work, PbO_2 was used as the starting material to take into account the effect of lead polyvalency which has been ignored in previous studies.

EXPERIMENTAL TECHNIQUES

NH_4VO_3, supplied by VEB Laborchemie Apolda, East Germany, was used to prepare V_2O_5. Figure 2 shows the combined DTA, TG and DTG results obtained on heating pure NH_4VO_3 in the derivatograph (a simulta-

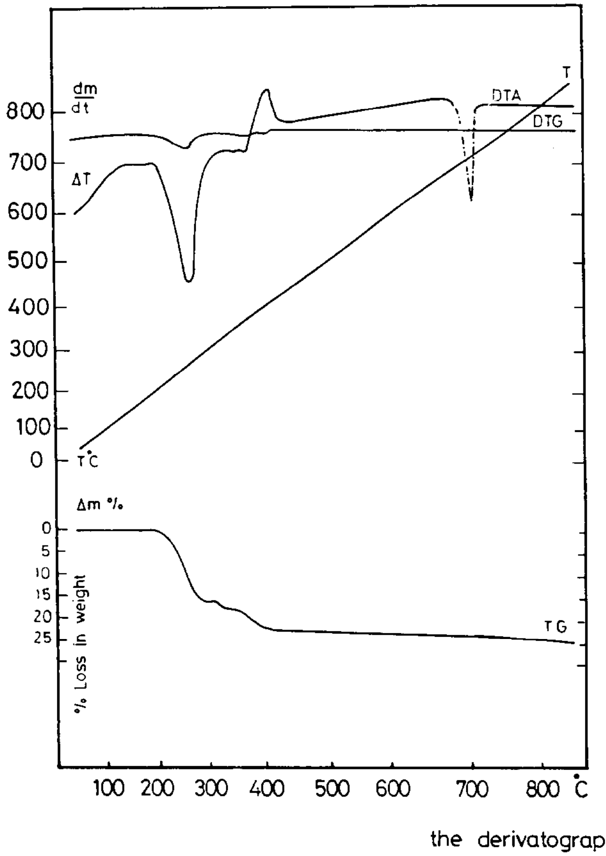

Fig. 2. Thermal analysis of NH_4VO_3 on the derivatograph (rate of heating 10 °C min^{-1}).

neous thermal analyser) at a heating rate of 10 °C min^{-1} in a Pt crucible. Conversion to V_2O_5, demonstrated by constant weight, occurs at about 400 °C. The DTA peak at 700 °C corresponds to the melting of the oxide. In view of these curves, V_2O_5 was prepared by heating NH_4VO_3 at 600 °C to a constant weight.

PbO_2 (A.R) grade was also supplied by VEB Laborchemie Apolda, and was found to contain 0.7% maximum impurities. PbO_2 was dried at 120 °C prior to weighing out the appropriate amounts of V_2O_5 and PbO_2 and mixing them in an agate mortar. The mixtures were then suspended in the thermobalance and the temperature raised to 120 °C until constant weight was obtained, in order to eliminate the moisture. The mixtures were then heated at different temperatures until equilibrium was reached at each temperature in order to determine the change in O/V ratio in each case. Such a technique has been extensively used to establish non-condensed systems [17,19,20].

EXPERIMENTAL RESULTS AND DISCUSSIONS

The dissociation curves for several mixtures were used to draw the ternary isobaric diagram in air shown in Fig. 3. These results were confirmed by occasional DTA and TG analyses, as well as by X-ray diffraction analysis. The interpretation of the different dissociation curves can be made by considering these curves together with the ternary isobaric section, Fig. 3.

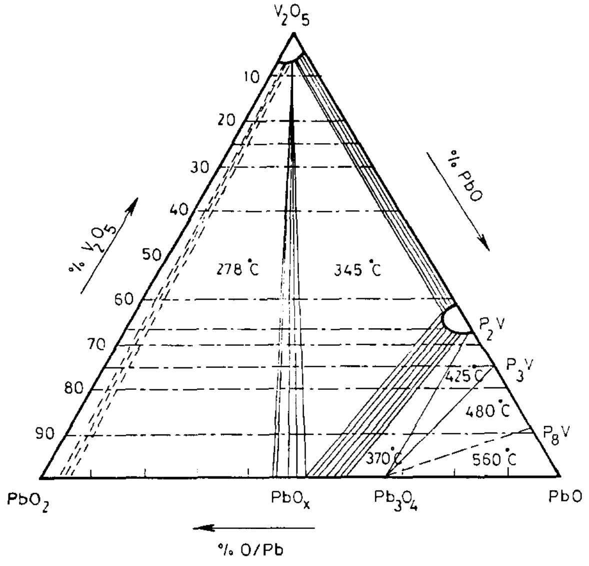

Fig. 3. Ternary isobar in air for the PbO_2–PbO–V_2O_5 system (molar basis).

Dissociation curves in air

All the dissociation curves show the following common characteristics. Oxygen is lost from about 100 to 278° C at which a vertical isothermal step occurs. Above 278° C, oxygen is progressively lost up to about 345° C at which a second vertical isothermal step is observed. However the extent of oxygen loss due to that step and, consequently, the location of the final compositions obtained on the ternary diagram depend on the composition of the original mixture. Accordingly, the different dissociation curves were divided into 4 groups.

Group 1. Dissociation curves for mixtures containing more than 33% V_2O_5 (molar)

Figure 4a was selected to show the main features observed in these mixtures. It shows the dissociation curve in air for a mixture initially

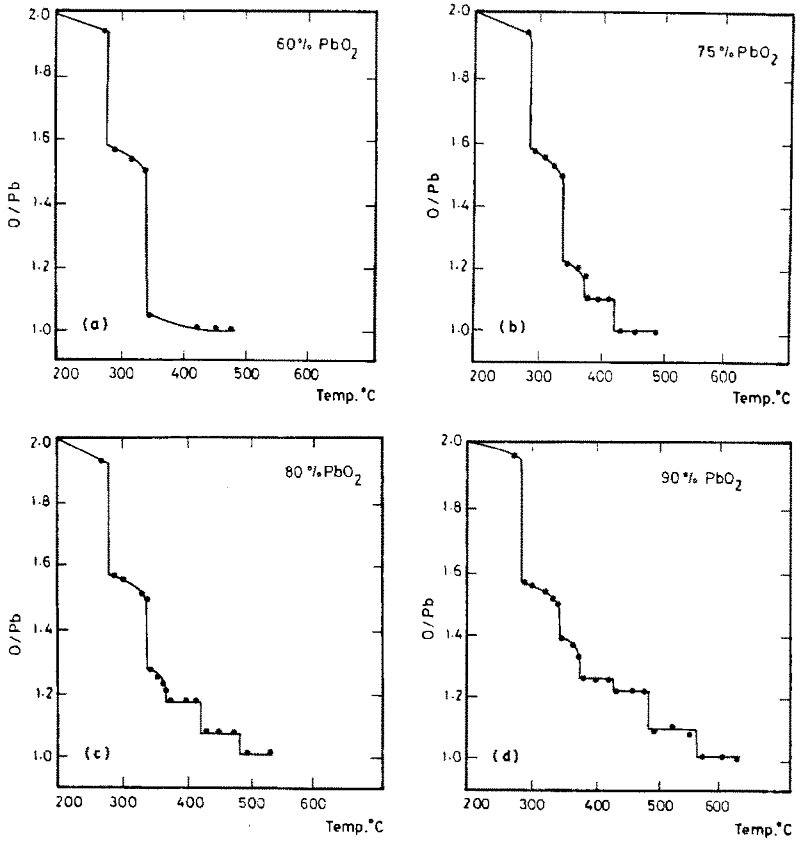

Fig. 4. Dissociation curve of (a) PbO_2–V_2O_5 mixture in air for $PbO_2 : V_2O_5 = 3 : 2$ (molar), (b) PbO_2–V_2O_5 mixture in air for $PbO_2 : V_2O_5 = 7.5 : 2.5$ (molar), (c) PbO_2–V_2O_5 mixture in air for $PbO_2 : V_2O_5 = 4 : 1$ (molar), and (d) PbO_2–V_2O_5 mixture in air for $PbO_2 : V_2O_5 = 9 : 1$ (molar).

containing 40% V_2O_5. As previously stated, at 278 °C a vertical step occurs corresponding to the reaction

$$PbO_x(s.s.) \rightarrow PbO_x(s.s.) + (2 - x/2)O_2 \quad (1)$$

Progressive oxygen loss then takes place until 345 °C where a vertical isothermal step takes the O/Pb ratio to about 1.05. On further temperature increase, the ratio approaches 1 at 420 °C. As seen from Fig. 3 the last vertical step corresponds to the reaction

$$2PbO_x(s.s.) + V_2O_5 = 2PbO \cdot V_2O_5(s.s.) + (x - 1)O_2 \quad (2)$$

The value of x at which this transition occurs was found to be about 1.48 for all mixtures.

Group 2. Dissociation curves for mixtures containing 25–33% V_2O_5 (molar)

Figure 4b shows the dissociation curves obtained on heating a mixture of PbO_2 and V_2O_5 containing 25% V_2O_5 (molar) under equilibrium conditions in the thermobalance: it shows the main features observed for all mixtures having a V_2O_5 content from 25 to 33%.

As seen from this figure, the step at 278 °C is followed by progressive oxygen loss until 345 °C at which a vertical step occurs. This step, as previously mentioned, corresponds to the formation of $2PbO \cdot V_2O_5$. However, the O/Pb ratio reached a value of 1.21. As shown in Fig. 3, at this temperature PbO_x coexists in equilibrium with $2PbO \cdot V_2O_5$. Progressive oxygen loss then takes place up to about 370 °C where a sudden vertical step indicates the formation of Pb_3O_4 according to the reaction

$$3PbO_x \rightarrow Pb_3O_4 + (3x - 4/2)O_2 \quad (3)$$

The O/Pb ratio remains constant up to about 425 °C, at which a final step occurs shifting the O/Pb ratio to 1. As seen in Fig. 3, this step corresponds to the reaction

$$2PbO \cdot V_2O_5 + \tfrac{1}{3}Pb_3O_4 \rightarrow 3PbO \cdot V_2O_5 + \tfrac{1}{6}O_2 \quad (4)$$

Evidence of the formation of $3PbO \cdot V_2O_5$ at such low temperatures was obtained by X-ray analysis, as will be discussed later.

Group 3. Dissociation curves for mixtures containing 11–25% V_2O_5 (molar)

Dissociation curves of a mixture containing 20% V_2O_5 is shown in Fig. 4c. The O/Pb ratio varies in almost the same way as the 25% V_2O_5 mixture, i.e. the invariant situations observed at 278, 345 and 370 °C are present. At the end of the step at 425 °C, the O/Pb ratio is 1.09. This ratio remains constant up to about 480 °C where a sudden loss changes the O/Pb ratio to unity. This loss in weight corresponds to the reaction

$$3PbO \cdot V_2O_5 + \tfrac{5}{3}Pb_3O_4 \rightarrow 8PbO \cdot V_2O_5 + \tfrac{5}{6}O_2 \quad (5)$$

Group 4. Dissociation curves for mixtures containing up to 11% V_2O_5 (molar)
Figure 4d shows the dissociation curve for a mixture initially containing 10% V_2O_5. The invariant situations are observed once more at the same temperatures of 278, 345, 370, 425 and 480 ° C, as seen by the corresponding vertical steps. At the end of the step at 480 ° C, the O/Pb ratio is about 1.1 and remains constant up to 560 ° C where it drops suddenly to unity. This temperature is the same temperature at which pure Pb_3O_4 transforms to PbO [17] indicating that PbO does not take V_2O_5 into solid solution.

Combined thermal analysis results

Figure 5 shows the combined DTA, TG and DTG results obtained by heating a mixture initially containing 66% PbO_2 (molar). The thermal curves obtained are as expected in view of the results of the equilibrium dissocia-

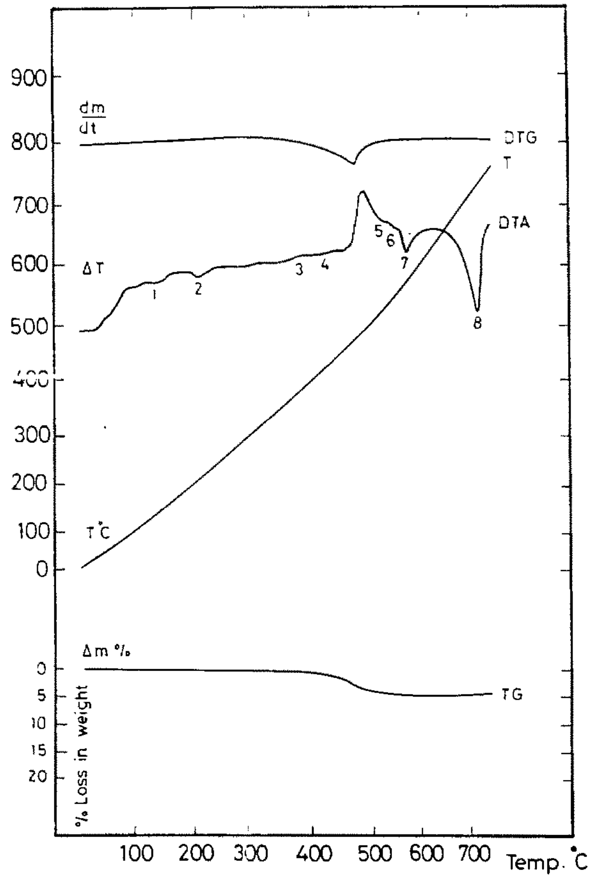

Fig. 5. Thermal analysis of $2PbO_2 : V_2O_5$ (molar) on the derivatograph (rate of heating 10 ° C min^{-1}).

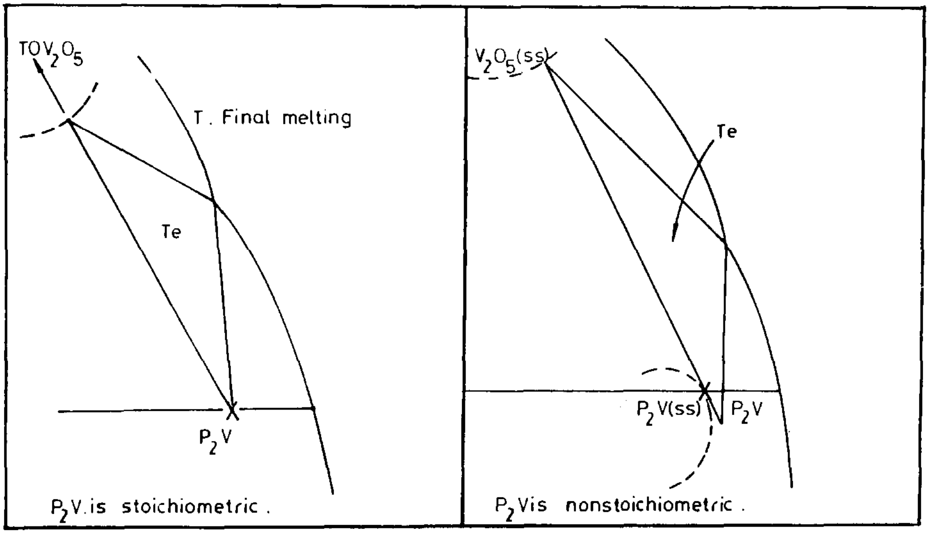

Fig. 6. Non-stoichiometry of $2PbO \cdot V_2O_5$.

tion curves. In particular, the presence of peak 7 on the DTA which is not accompanied by a change in weight (on the TG and DTG curves), seems to be in favour of the assumed formation of a solid solution of $2PbO \cdot V_2O_5$. If $2PbO \cdot V_2O_5$ was a stoichiometric phase then it would have melted at a definite temperature without any trace of liquid appearing before melting. In that case, we should have obtained one melting peak on the DTG. The fact that peaks 7 and 8 occur without weight change means that melting has occurred over a range of temperatures. This could be the case if $2PbO \cdot V_2O_5$

TABLE 3

Combined thermal analysis of a mixture containing $2PbO_2 : V_2O_5$ (molar)

Peak number	Type	Temperature (°C)	Change in weight	Interpretation
1	endo	140	slight	Loss of moisture
2	endo	220	slight	Non-stoichiometry of PbO
3	endo	390	yes	Transition to PbO_x
4, 4′	endo	420–460	yes	Non-stoichiometry of PbO_x
5	endo	520	yes	Transition to $2PbO \cdot V_2O_5$
6	endo	540	slight	Non-stoichiometry of $2PbO \cdot V_2O_5$
7	endo	570	no	Eutectic formation between $2PbO \cdot V_2O_5$(s.s.) and V_2O_5(s.s.)
8	endo	720	no	Congruent melting of $2PbO \cdot V_2O_5$

is a non-stoichiometric phase. This situation is shown in Fig. 6. Being performed under non-equilibrium condition (heating rate of 10 °C min^{-1}), the combined thermal curves gave transition temperatures higher than the corresponding equilibrium temperatures. Table 3 summarizes the results of the combined thermal analysis.

The ternary isobaric section in air

Figure 3 shows the ternary isobaric section obtained by plotting the beginning and the end of each step obtained on the dissociation curves. The following invariant situations occur.

(i) At 278 °C, PbO_2(s.s.), V_2O_5(s.s.) and PbO_x ($x = 1.57$) coexist with oxygen in equilibrium. The composition of the V_2O_5(s.s.) vertex of the tie triangle V_2O_5–PbO_x–PbO_2 is not certain. That is why the tie lines joining PbO_2 and V_2O_5(s.s.) as well as the small solid gap at the V_2O_5 vertex are shown dotted in the figure.

(ii) At 345 °C, PbO_x ($x = 1.5$), V_2O_5(s.s.) and $2PbO \cdot V_2O_5$(s.s.) coexist in equilibrium with oxygen. The presence of both V_2O_5(s.s.) and $2PbO \cdot V_2O_5$(s.s.) were confirmed by X-ray analysis as well as by joining compositions reached at the same temperature on the ternary phase diagram (as will be explained when discussing the monovariant situation). The occurrence of this tie triangle implies that the use of PbO_2 (instead of PbO) resulted in the formation of $2PbO \cdot V_2O_5$ at 345 °C instead of 600 °C which was reported when PbO was used [11]. This is due to the destabilization of PbO_x by reaction with V_2O_5.

(iii) At 370 °C, PbO_x ($x = 1.41$, $2PbO \cdot V_2O_5$(s.s.) and Pb_3O_4 coexist in equilibrium with oxygen. This is almost the same temperature at which pure PbO_x converts to Pb_3O_4 implying that neither of the two oxides has taken $2PbO \cdot V_2O_5$ into solid solution.

(iv) At 425 °C, $2PbO \cdot V_2O_5$(s.s.), $3PbO \cdot V_2O_5$ and Pb_3O_4 coexist in equilibrium with oxygen. Hence 425 °C can be considered as the minimum temperature required for the preparation of $3PbO \cdot V_2O_5$. The formation of $3PbO \cdot V_2O_5$ was confirmed by X-ray analysis.

(v) At 480 °C, $3PbO \cdot V_2O_5$, Pb_3O_4 and $8PbO \cdot V_2O_5$ coexist in equilibrium with oxygen. In view of the absence of X-ray data concerning $8PbO \cdot V_2O_5$, this compound could not be identified by X-ray analysis. The dissociation curve of the mixture initially containing 90% PbO_2 showed a slight O/Pb drop at 480 °C giving a value of O/Pb at the termination of this step of 1.1. This composition almost lies on a tie line joining Pb_3O_4 and $8PbO \cdot V_2O_5$ suggesting the presence of this latter compound. In view of this result and the work of previous authors, it was placed on the V_2O_5–PbO edge and the tie line joining this compound to Pb_3O_4 was shown dotted.

(vi) At 560 °C, $8PbO \cdot V_2O_5$, Pb_3O_4 and PbO coexist in equilibrium with oxygen. This temperature is identical to the temperature at which the

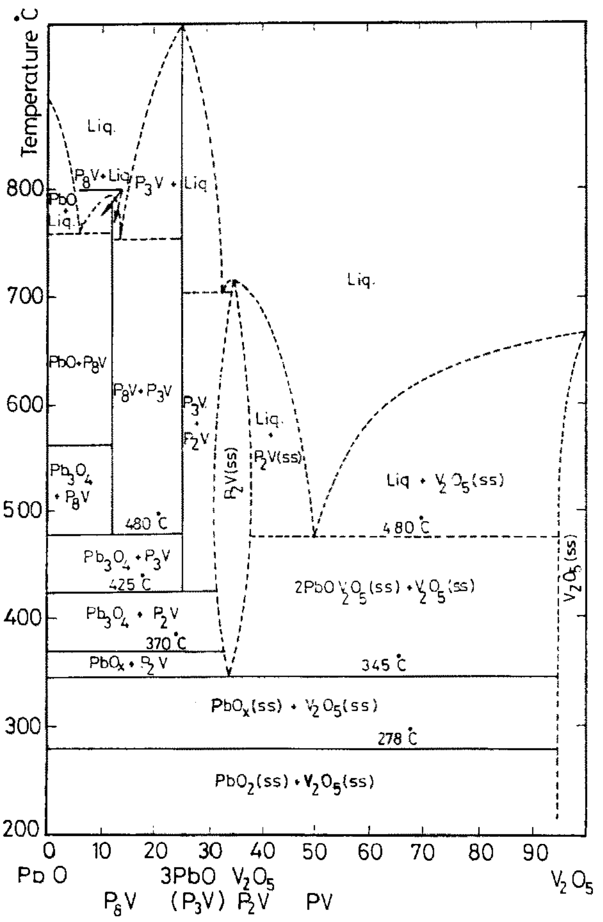

Fig. 7. Quasi-binary isobaric section in air for the system PbO_2–PbO–V_2O_5 (ss, solid solution).

decomposition of Pb_3O_4 to PbO occurs in the case of pure oxides, implying that PbO does not take any V_2O_5 into solid solution.

The following three monovariant situations (where 2 solid phases coexist in equilibrium with oxygen) exist.

(1) At temperatures ranging from about 100 to 278 °C, PbO_2 coexists in equilibrium with V_2O_5(s.s.). The tie lines are shown dotted as previously explained.

(2) At temperatures ranging from 278 to 345 °C, PbO_x $(1.5 < x < 1.57)$ coexists in equilibrium with V_2O_5(s.s.) and oxygen.

(3) At temperatures ranging from 345 to 370 °C, PbO_x $(1.41 < x < 1.5)$ coexists in equilibrium with $2PbO \cdot V_2O_5$ and oxygen. Evidence for the presence of this series of tie lines is obtained from the slight progressive loss in weight observed in the dissociation curves corresponding to compositions containing more than 66% PbO_2 (molar) between 345 and 370 °C. When the

O/Pb ratios corresponding to the beginning and end of the progressive weight-loss region on the dissociation curves are projected on the ternary diagram, the points existing at the same temperatures are colinear with PbO_x and $2PbO_x \cdot V_2O_5$ for values of x ranging from 1.5 to 1.41, and for compositions of $2PbO \cdot V_2O_5$ containing a higher proportion of oxygen than the stoichiometric ratio.

Two regions of solid solutions appear on the ternary diagram: V_2O_5(s.s.) the presence of which was confirmed by X-ray diffraction analysis although the extent to which this phase can take lead oxides in solid solution is uncertain; and $2PbO \cdot V_2O_5$(s.s.) which was confirmed by X-ray diffraction. Also, the presence of the solid solution containing excess oxygen was suggested by the location of the tie lines representing V_2O_5–$2PbO \cdot V_2O_5$ and $2PbO \cdot V_2O_5$–PbO_x. A projected quasi-binary temperature-composition diagram is shown in Fig. 7.

X-ray results

The V_2O_5 solid solution

Identification of a solid solution using X-ray diffraction relies on the slight shift in the *d*-spacings of the compound which occurs as the solid

TABLE 4

X-ray results for V_2O_5 and V_2O_5(s.s.)

V_2O_5 (pure)		V_2O_5 95%–PbO_2 5%	
d	I/I_0	*d*	I/I_0
–	–	7.25	100
5.76	40	5.79	10
4.38	100	4.37	61
4.05	35	4.10	20
3.40	90	3.38	30
2.88	65	2.89	22
2.76	35	2.77	8
2.69	75	2.68	7
2.61	40	2.61	12
2.492	7	2.49	8
2.405	7	2.39	9
2.185	17	2.18	32
2.042	3	2.03	6
1.992	17	1.98	12
1.910	25	1.92	11
1.900	17	1.90	10
1.864	13	1.87	14
1.757	30	1.76	8
1.564	11	1.58	9
1.540	3	1.54	14
1.515	17	1.51	9
1.493	17	1.49	13

TABLE 5

X-ray diffraction pattern of $2PbO \cdot V_2O_5$

d	I/I_0	d	I/I_0 (from ref. 18)
6.92	8	6.89	52
4.35	23	4.38	100
3.69	11	3.64	85
3.60	47	3.58	29
3.45	100	3.46	29
3.22	97	3.21	57
–	–	3.15	23
3.10	55	3.12	47
3.00	34	3.01	33
2.94	17	2.93	32
2.75	22	2.75	34
2.65	7	2.66	23
–	–	2.60	14
2.42	9	2.42	27
2.28	19	–	–
2.24	22	–	–
2.18	20	–	–
2.09	23	–	–
1.83	17	–	–
1.73	14	–	–

solution is formed [21]. To confirm the presence of V_2O_5 solid solution, a mixture initially containing 95% V_2O_5 and 5% PbO_2 was heated for 48 h at 500 °C. A comparison between the lines obtained for pure V_2O_5 and those of the heated sample is shown in Table 4. As can be seen from this table, there is a slight shift in the values of the *d*-spacings indicating that up to at least 5% lead oxide can dissolve in V_2O_5.

The diffraction pattern of $2PbO \cdot V_2O_5$

A mixture initially containing 66% PbO_2 and 33% V_2O_5 (molar) was heated for 48 h at 510 °C and subjected to X-ray analysis. The X-ray pattern of the powder is presented in Table 5 and compared with the pattern reported by Baiocchi et al. [18]. From this table it appears that the lines obtained in the present study are very close to those recently reported in ref. 18, except for slight shifts in *d*-spacings denoting the formation of the proposed $2PbO \cdot V_2O_5$ solid solution. The presence of this solid solution led Baiocchi et al. [18] to conclude that this phase is richer in V_2O_5 content than $2PbO \cdot V_2O_5$. Five more lines also appeared which were identified as lines characteristic of Pb_3O_4. The presence of Pb_3O_4 is not surprising in view of the proposed formation of $2PbO \cdot V_2O_5$ solid solution rich in V_2O_5.

TABLE 6

Suggested X-ray diffraction pattern of $8PbO \cdot V_2O_5$

d	I/I_0
4.50	19
3.39	8
2.23	100
3.02	50
2.99	27
2.90	50
2.04	17
1.90	13
1.69	14

The diffraction pattern of 80% PbO_2–20% V_2O_5 (molar)

A mixture initially containing 80% PbO_2–20% V_2O_5 (molar) was heated to 560 °C for 48 h and subjected to X-ray analysis. The resulting peaks were compared with the *d*-spacings of $3PbO \cdot V_2O_5$ [22]. Most of the lines of $3PbO \cdot V_2O_5$ appeared. This suggests that the remaining lines correspond to $8PbO \cdot V_2O_5$. Table 6 shows the "screened" lines of $8PbO \cdot V_2O_5$.

CONCLUSIONS

From the isobaric sections constructed for the system PbO_2–PbO–V_2O_5, the following compounds have been established: $2PbO \cdot V_2O_5$(s.s.), $3PbO \cdot V_2O_5$ (P_3V) and $8PbO \cdot V_2O_5$ (P_8V) and their stability regions were determined. The previously reported compound $4PbO \cdot V_2O_5$ (P_4V) was not found to exist in air.

The minimum temperature required to obtain P_3V from $PbO_2 + V_2O_5$ is 425 °C and its presence was confirmed by X-ray analysis. X-ray data for P_8V were established.

There are six invariant situations established in air in this system. At the indicated temperatures, three solid phases coexist in equilibrium with oxygen.

(i) At about 278 °C, PbO_2(s.s.), V_2O_5(s.s.) and PbO_x ($x = 1.57$).

(ii) At 345 °C, PbO_x ($x = 1.5$), V_2O_5(s.s.) and P_2V.

(iii) At 370 °C, PbO_x ($x = 1.41$), P_2V(s.s.) and Pb_3O_4.

(iv) At 425 °C, P_2V(s.s.), P_3V and Pb_3O_4.

(v) At 480 °C, P_3V, Pb_3O_4 and P_8V.

(vi) At 560 °C, P_8V, Pb_3O_4 and PbO.

Also, three monovariant situations occurred where two solid phases and oxygen coexist in equilibrium:

(1) At temperatures ranging from 100 to 278 °C, PbO_2(s.s.) coexists in equilibrium with V_2O_5(s.s.) and O_2.

(2) At temperatures ranging from 278 to 345 °C, PbO_x $(1.5 < x < 1.57)$ coexists in equilibrium with V_2O_5 and O_2.

(3) At temperatures ranging from 345 to 370 °C PbO_x $(1.41 < x < 1.5)$ coexists in equilibrium with P_2V and O_2.

Two regions of solid solutions appear on the ternary diagram:

(a) V_2O_5(s.s.), the presence of which was confirmed by X-ray identification.

(b) P_2V(s.s.) containing a higher proportion of O_2 than the stoichiometric ratio, the presence of which was also confirmed by X-ray analysis.

REFERENCES

1 Tokyo Shibaura Elect. Co. Ltd., Japan, Report 81-26-746 (Cl. C03C3/30), March 1981.
2 E.P. Denton, H. Rauson and J.E. Stanworth, Nature, 173 (1964) 1030.
3 A.T. Andreeva, M.N. Verebeichick, P.G. Zhuravleva and D.I. Fridbery, Nov. Neor. Stekl. Matter, 41 (1979).
4 S.P. Parker (Ed.), McGraw-Hill Encyclopedia of Science and Technology, Vol. 8, 1987, p. 125.
5 Y. Asahara, Hoya Glass Works Ltd., Japan Kokai; 77-69-916 (Cl. C03C3/16), June 1977.
6 V.Z. Petrova, I.V. Filatova, P.E. Kandyba, I. Vazhenin, G.I. Vadov and Yu. Ku. Znetsov, Moscow Inst. of Elect. Technology, U.S.S.R. Patent No. 614-039, July 1978; Chem. Abstr., 89 (1978) 94044e.
7 Yu. Goltsov, L.A. Belova, V.P. Cherpillo, V.T. Maltsev and O.I. Prokopalo, Rostov St. Univ., U.S.S.R. Patent No. 667-530, May 1979; Chem. Abstr., 90 (1979) 82153t.
8 V.M. Nogiev, Ah. Fiz. Chim., 52(7) (1978) 174.
9 M.M. Ahmed and C.H. Hogarth, J. Mater. Sci., 18(11) (1983) 3305.
10 S. Yatabe and S. Kunimoto, Yasmaguchi Daigaku Kogakubu Kenkyu Hokoku, 31(2) (1981) 333; Chem. Abstr. 95 (1981) 106929m.
11 T. Tokokawa and O.J. Kleppa, Inorg. Chem., 3(7) (1964) 954.
12 M. Amadori, Ann. Inst. Veneto Sd., 76 (11) (1917) 419.
13 G. Simon and S.L. Ardelean, Ser. Chem., 15(11) (1970) 43 (in Romanian).
14 R.F. Geller and E.N. Bunting, J. Res. Nat. Bur. Stand., 18 (1937) 585.
15 I.A. Vasilieva, S.M. Mudrestova and L.V. Stesikova, Ser. Khim., 21(6) (1985) 47 (in Russian).
16 T. Shimohira, S. Iwa and H. Tagai, Vozyo Kyokai Shi, 75(868) (1967) 350 (in Japanese).
17 M.F. Abadir, A.M. Gadalla and Y.M. Agamawi, J. Trans. Brit. Ceram. Soc., 75(4) (1976) 68.
18 E. Baiocchi, M. Bettinelli, A. Monteners and I. Disipio, J. Solid State Chem., 43(1) (1982) 63.
19 R. El-Shahat, A.M. Gadalla and J. White, in G. Steward (Ed.), Science of Ceramics, Vol. 3, Academic Presss, London, 1967.
20 A.M. Gadalla and M.F. Abadir, Ind. Eng. Chem. Fundam., 23(2) (1984) 220.
21 B.D. Cullity, Elements of X-ray Diffraction, Addison–Wesely, 1959.
22 ASTM X-ray Card No. 11-471.